

An Innovative Fault Context Identification Algorithm for High Speed Distance Protection

Ujjaval J. Patel, Nilesh G. Chothani, Praghnes J. Bhatt

Article Info

Volume 82

Page Number: 15824 - 15831

Publication Issue:

January-February 2020

Abstract:

The main aspects influencing the transmission line protection are fault impedance, Load Angle (LA), Fault Application Angle (FAA), Location of fault (FL) and Fault Type (FT). The conventional DFT algorithm used for the phasor measurement removes only integer harmonics and speed of the algorithm is also not sufficient to meet the critical relaying requirement. In this paper, an adaptive algorithm is presented for fast and accurate estimation of Fault Location and classification based on Modified Fourier Transform (MFT). Simulations have been performed in PSCAD to obtain the fault signatures during various fault scenario. The developed test algorithm is scripted in MATLAB followed by validation during extreme faulty conditions. It has been found that the proposed algorithm effectively filters the harmonics, decomposes the fundamental signal from the complex waveforms and operates precisely within one cycle time required for high speed distance protection.

Keywords: Fault location; Impedance reach; Modified Fourier Transform (MFT); Numerical relaying; Transmission Line Protection.

Article History

Article Received: 18 May 2019

Revised: 14 July 2019

Accepted: 22 December 2019

Publication: 28 February 2020

I. INTRODUCTION

Fast and accurate numerical relaying algorithm are used in present era for phasor computation of analog signals in order to minimize impacts of disturbance and enable the system restoration. To satisfy these, the protection and control actions must be designed and coordinated properly [1]. The major disturbances can be identified as “hidden fault signatures” in relay itself which can be undetected by conventional relays during extreme fault scenario. Nevertheless, it can be minimized by most of the numerical relays [2]. Reliable and secure protection for transmission line is essential for maintaining dynamic stability and uninterrupted power demand [3]. In practice, transmission line is protected by classical relaying techniques such as distance protection, carrier aided protection, over current relays etc. Directional protection is also used to protect the ring main systems to improve the reliability. Carrier aided scheme is most popular and widely used for transmission line protections but it gives the delayed tripping and incorrect phasor estimation due to varying system disturbances. As a remedy of this, distance protection can be used for

fast and accurate protection scheme. Nowadays, many filtering techniques are existing for reliable and quick relay response [4]-[6]. The major issues with such algorithms are estimation error and slow response due to effect of DC & harmonic components. Some algorithms implement filters like Walsh, Kalman, LSE and mimic filtering [6]-[10] but they suffer from the setback of sluggish convergence response. Other methods based on “Artificial Neural Networks (ANN)” [11]-[14] have been demonstrated by many research fellows, but the algorithms with ANN configuration requires sufficient training data for fast fault detection and hence requires large memory. For the algorithm based on “Mathematical Morphology (MM)” [15], imposes computational burden. The next section covers system modeling for evaluation of developed scheme in PSCAD followed by proposed algorithm in Section III which contains phasor estimation technique, impedance reach measurement with detection & classification of fault. Results of the developed algorithm are compared with existing algorithms as discussed in Section IV.

II. PSCAD TEST SYSTEM

A portion of Indian power grid network connected by two generators through a common transmission line is shown Fig. 1. The synchronous generators and power line data are specified in Appendix A. System voltages and currents are measured at the generator G1 using bus CTs and line PTs with sampling frequency of 4kHz.

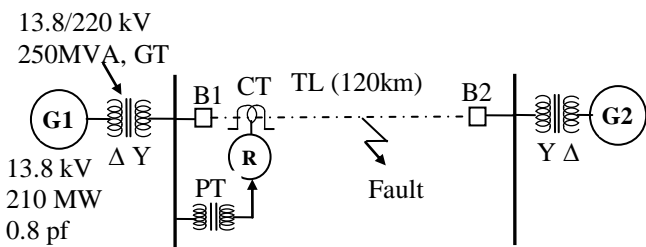


Fig. 1: Modeling of test system in PSCAD

The modelled system has been tested for all 10 types of faults at various locations along the line starting from the relay location including close in fault to boundary end faults. Further, faults are applied with variable different fault application angles (0° , 10° , 30° , 45°) and load angle (0° , 5° , 8°). The load in power grid has been regulated by tuning the load angle between the two generating stations. Around 1500 simulation cases are generated with varying system parameters using Multiple-run features existing in PSCAD and the same are extensively validated using proposed algorithm designed in MATLAB software. Error in estimation of fault locations are found within 1.23% with accurate classification of fault type.

III. PROPOSED TECHNIQUE

Fig. 2 shows proposed distance relaying algorithm as applied to numerical relaying application. The three phase voltage & current data are extracted using PSCAD and phasor estimation of these input signals can be done using conventional DFT algorithm. The prime application of digital filter algorithm for numerical relaying is to remove the decaying DC component and harmonics to minimize system oscillations and to estimate exact fundamental

complexphasors.

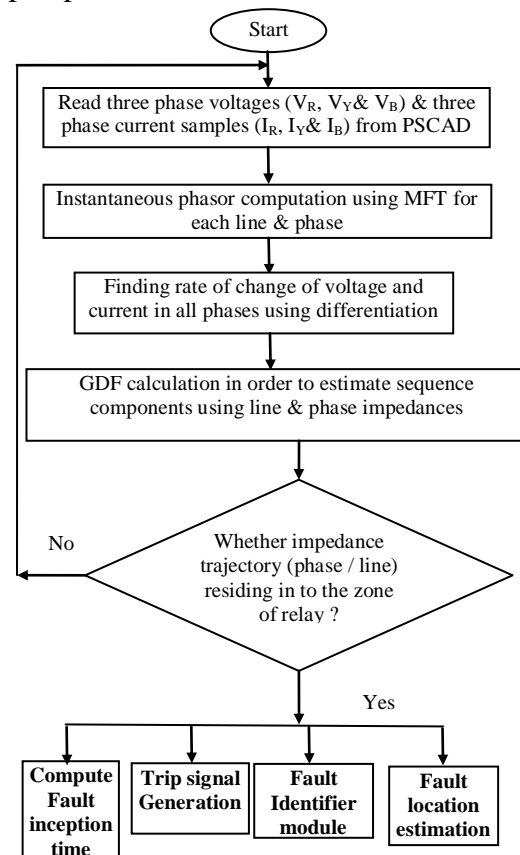


Fig. 2: Proposed Distance Relaying Algorithm

Let us consider a sinusoidal signal $x(t)$ having fundamental period T sampled with a sampling rate of N times and hence sampling period will be $\Delta T = T/N$. In the proposed MFCDF, the magnitude and angle of input signal $x(t)$ are calculated which yields in complex phasor estimation. Using MFCDF, real and imaginary part of the $x(t)$ are calculated for each sample. Algorithm is executed to calculate phasors of both voltages and current signals, simultaneously using the equations:

$$X_{r1}(N) = X_r(N) - \frac{2}{N} \sum_{k=1}^N \left(D e^{-\frac{k\Delta T}{\tau}} + D_1 e^{-\frac{k\Delta T}{\tau_1}} \right) \cos\left(\frac{2\pi k}{N}\right) \quad (1)$$

$$X_{i1}(N) = X_i(N) - \frac{2}{N} \sum_{k=1}^N \left(D e^{-\frac{k\Delta T}{\tau}} + D_1 e^{-\frac{k\Delta T}{\tau_1}} \right) \cos\left(\frac{2\pi k}{N}\right) \quad (2)$$

Where, r = real part, i = imaginary part, k = samplenumber, τ = time constant of the line = L/R , τ_1 = time constant of the digital filter, D & D_1 are filter parameters which can be found as outlined in [5]. The magnitude & phase angle can be computed with help of equations,

$$|X(j, N)| = \sqrt{(X_{r1}(j, N))^2 + (X_{i1}(j, N))^2} \quad (3)$$

$$\angle(X(j, N)) = \tan^{-1}\left(\frac{X_{i1}(j, N)}{X_{r1}(j, N)}\right) \quad (4)$$

These equations yield phasors of j^{th} input signal at N^{th} instance. Apart from these, it also gives maximum magnitude and angle of applied analog signals. The root mean value can be computed using,

$$M_j = X(j, N) = \frac{|X(j, N)|}{\sqrt{2}} \quad (5)$$

Expressions (4) & (5) extracts the phase & RMS magnitude of fundamental signal from the original complex phasor after removal of harmonics components and decaying DC, which indicate its efficacy for numerical relaying applications. Extracted phasors further applied to current differential algorithm which accurately detects the fault condition for issuing the trip signal for actuating the circuit breaker. For the different fault condition, especially high resistance fault; the fault current is significantly affected due to the presence of high fault impedance. In such cases the proposed algorithm is very effective as it operates on the measurement of differential current phasor for generating the relay trip signal. On the other hand, power swing condition can be detected with the use of proposed algorithm with the additional signal of differential voltage phasors. Also the algorithm is able to estimate the time at which the fault occurs, hence its application can be extended for the phasor measurement unit for further recording of the signals. After issuing of trip signals from relay, the

phasor values of bus voltages and line currents are also applied for the sequence component block which is separating zero, negative and positive sequence elements. The output of sequence components are used for estimating the phase impedance and line impedances. The phase faults are estimated by mapping the same in phase impedance planes and line faults are estimated by mapping line impedance in line impedance planes of relays. The calculated phase and line impedances are compared with the set value of quadrilateral characteristics to detect the faults. The impedance trajectory and magnitude of impedance will decide the location, direction and types of the fault occurred on transmission line. In this paper, different kinds of faults are generated in PSCAD and the current and voltage signals are captured using multiple run feature available in EMTDC. Then subsequent analysis for verifying the fault contexts are scripted and validated in MATLAB. The proposed algorithm can also be implemented in advanced controller or Digital Signal Processor (DSP) for realizing actual MFCDF based phasor estimation and numerical relaying. The main advantages of this algorithm are that apart from accurate and fast phasor estimation, it also calculates fault time, identifies type of fault and location of fault which is very much helpful to power system engineers. The different types of faults are simulated in PSCAD and a comparison of the results for conventional DFT based phasor estimation and MFCDF based phasor estimation are given in next section.

IV. RESULTS & DISCUSSION

The response of phasor estimation by scripting the logics for DFT and MFT are demonstrated in Fig. 3. Responses are compared by simulating the model test system presented in section II using PSCAD for line to ground fault applied at 400 sample number. The effect of DC component and magnitude are maximum when the fault has been applied with application angle of 0° . The obtained responses signpost that projected phasor assessment method accomplishes phasor estimation of faulted signals in

a superior manner in comparison with orthodox DFT with the removal of harmonics and influencing DC component. Signal processing for magnitude and phase yields proper impedance response for each fault cases with power system disturbances.

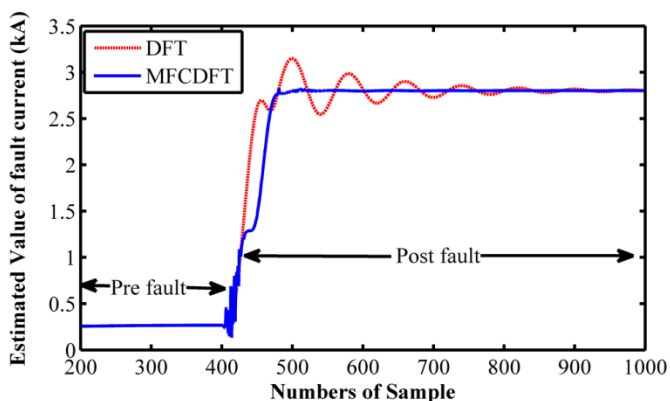


Fig. 3: Phasor computation for fault current

using MFT and DFT during phase fault applied at 400 sample number with Fault Application Angle of 0°

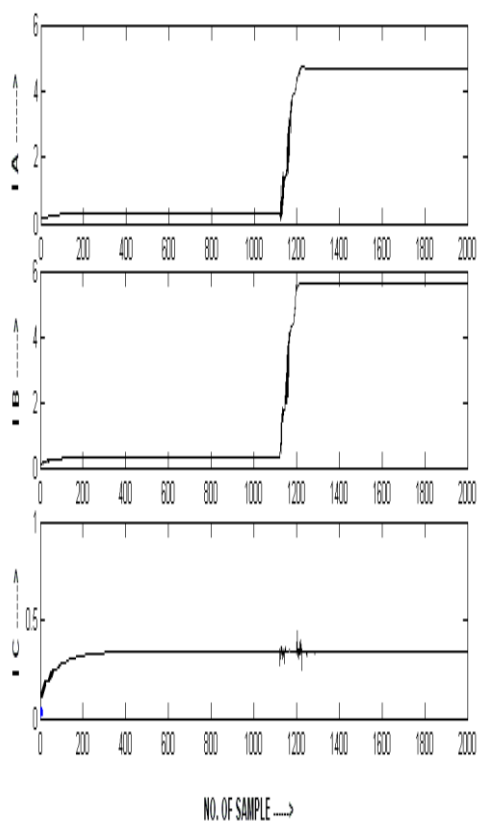


Fig. 4: Current Phasors Estimation using MFT

Fig. 4 demo graphs phase current magnitude estimations for each phase during AB-G fault applied at 0.285 second (1140 sample). It is observed that the magnitude of current phasor in phase A and B increases to a very high value with occurrence of AB-G fault whereas the magnitude of current phasor in phase C remains unaffected.

Table - I: Summary of Test Results of Phasor Estimation

Algorithm	Filter Order	Estimation Value	Estimation Error
Conventional FCDFDFT	1	$I = 32510 \text{ A}$ $\Theta = -75.76^\circ$	0.26% 2.26%
Conventional FCDFDFT	2	$I = 73102 \text{ A}$ $\Theta = -36.05^\circ$	0.31% 0.91%
Modified FCDFDFT	1	$I = 32518 \text{ A}$ $\Theta = -75.82^\circ$	0.00% 0.01%
Modified FCDFDFT	2	$I = 73126 \text{ A}$ $\Theta = -36.56^\circ$	0.00% 0.00%

A comparison of phasor estimation using conventional DFT based algorithm and MFCDFDFT based algorithm is done after implementing first order and second order filter and it is shown in Table - I. It is shown that for the type-2 digital filter, modified full cycle discrete Fourier transform based algorithm is very accurate and shows satisfactory results. The output of phasor estimation block is applied to voltage and current differential algorithm and the main relaying decision is taken to trip the circuit breaker. The results of current differential algorithm during high resistance fault (15Ω) are shown in Fig. 5 for AB-G fault applied at 0.28 second. The advantage of using the differential current phasor algorithm is clearly visible in Fig. 5, as the reduction of the current magnitude due to the presence of high fault resistance changes current magnitude equally in respective phase. Hence, the difference in current phasor eliminates the error introduced due to high resistance fault. Fig. 5 clearly shows that for AB-G fault, the difference of current A-B is very small in case of AB.

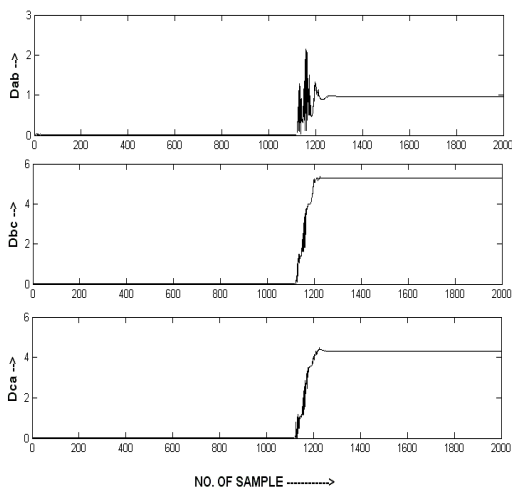


Fig. 5: Differential Current Phasors

modules are Trip_A, Trip_B & Trip_C and for line modules are Trip_AB, Trip_BC & Trip_CA respectively. All fault identifier modules are realized so that if impedance locuses are falling in to the trip region of quadrilateral characteristic, then its output makes transition to 1(high) else it stays at 0 (low).

Fig. 6 represents the response of the relay during AB-G fault which occurs at 1140 samples. It is also shown that the relay fails to operate on high resistance AB-G fault due to incorrect estimation of fault current with conventional DFT. The locus of the line & phase impedances are presented in Fig. 7 and Fig. 8 respectively for this same fault condition. It is clearly observed that the impedance locus does not enter into the relay characteristic even in case of fault and relay results in mal operation. It is observed that line & phase impedance locus are falling outside the relay characteristics and results in under reach operation. Fig. 9 shows the waveform of voltage and current waveforms and based on these signals, differential current phasor are calculated based on proposed MFCDFT algorithm for generating relay trip signal. The impedance locus measured with the use of this differential current phasor is represented in Fig. 10 & Fig. 11. The proposed algorithm can accurately compute the impedance and hence its locus enters into the operating boundary of relay for its correct tripping. Fault identifier modules are designed to identify type of fault occurred in the power system depending on the type of impedance locus entering into the trip region. In fault identifier, impedance modules are realized for each phase & line resulting in six identical modules, each for phase to ground fault (A-G, B-G & C-G) and for line-to-linefault (AB, BC & CA). The response signals of phase

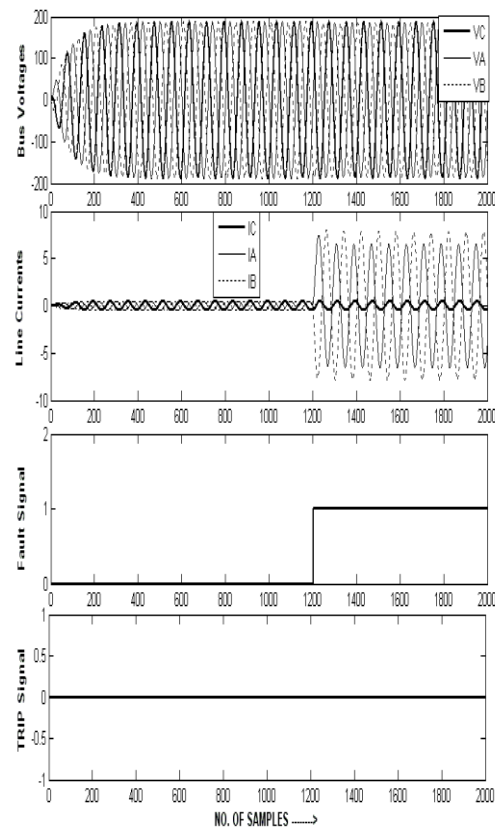


Fig. 6: Wave forms during high resistance (15 Ω) AB – G fault using conventional DFT

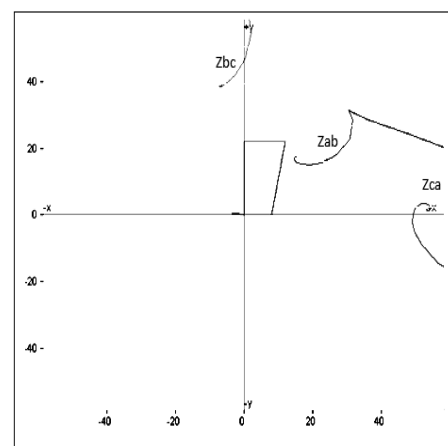


Fig. 7: Line Impedance trajectory using DFT

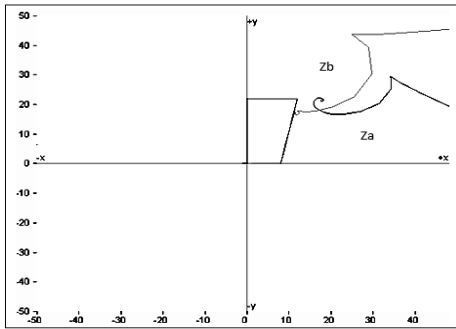


Fig. 8: Phase Impedance trajectory using DFT

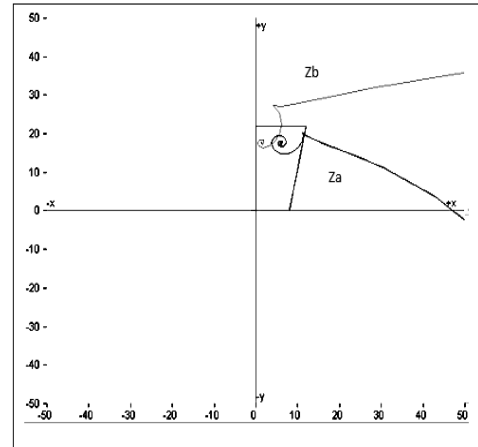


Fig. 11: Phase Impedance trajectory using MFT

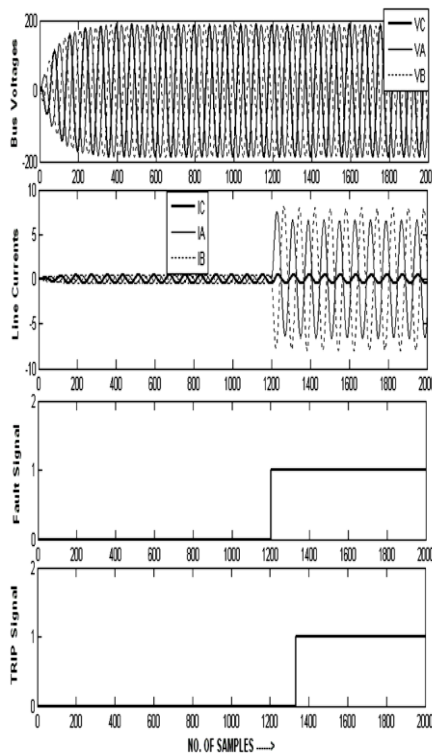


Fig. 9: Wave forms during high resistance (15 Ω) AB – G fault using Modified MFT

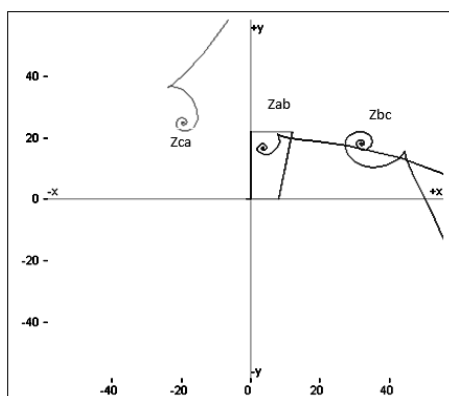


Fig. 10: Line Impedance trajectory using MFT

The responses of the fault identifier modules are tabulated in Table – II. From Fig. 9, it can be observed that for the BC-G fault incepted at 0.3 second, signals Trip_A, Trip_B and Trip_AB of the fault identifier module changes to followed by a of 12.5 ms which is within the one cycle time.

Table-II: Output of Fault Classifier for each type of fault

Cas e No.	Fault Incept ed	Trip_A	Trip_B	Trip_C	Trip_A	Trip_B	Trip_C	Fault Classif ied
1	A-G	1	0	0	0	0	0	A-G
2	B-G	0	1	0	0	0	0	B-G
3	C-G	0	0	1	0	0	0	C-G
4	AB	0	0	0	1	0	0	AB
5	BC	0	0	0	0	1	0	BC
6	CA	0	0	0	0	0	1	CA
7	AB-G	1	1	0	1	0	0	AB-G
8	BC-G	0	1	1	0	1	0	BC-G
9	CA-G	1	0	1	0	0	1	CA-G
10	ABC -G	1	1	1	1	1	1	ABC-G
1 : Fault is detected								0: Fault is not detected

The performance of developed algorithm reveals that it identifies type of fault with classification accuracy

of 100% with very fast response for all fault cases with power grid parameter ranges as presented in Section-II. The response of variation in fault location estimation error in veneration to fault impedance and location is demonstrated in Table-III for A-G fault applied with $FAA = 0^\circ$. The fault distance estimator scheme computes the distance of the fault by considering a ratio of calculated fault impedance to the unity impedance. The actual fault impedance has been calculated by the presented phasor computation algorithm and unit impedance is extracted from the acquaintance of X/R ratio of power system network to be safeguard. Location error can be computed with the formulae,

$$\% \text{ Error} = \frac{\text{Computed Location} - \text{Actual Location}}{\text{Actual Location}} * 100 \quad (6)$$

It can be summarized from the result investigation exemplified in Fig. 12 that in the course of close in faults up to 15km, the location error ranges within 1% and towards boundary end, it remains within $\pm 0.5\%$. Thus in comparison with prevailing schemes [10]-[11] in which optimal error in estimation is attained up to 5%, the error in fault distance judgment is considerably improved for wide range of fluctuation in fault distance, fault types and variation in fault impedances.

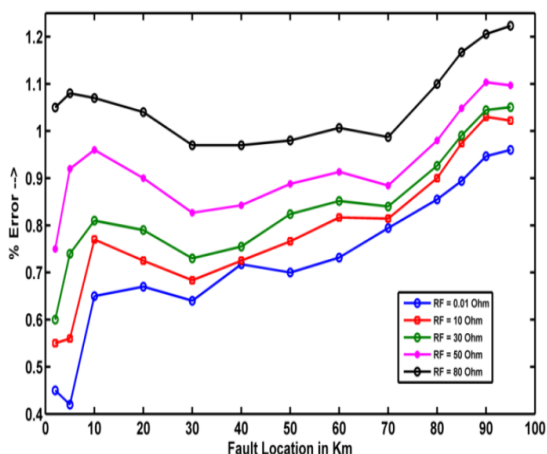


Table-III: Estimation of Fault Location for variation in fault resistance

Actual FL (Km)	Measured Fault Location (Km)				% Error in estimation of fault location			
	$R_F = 0.02 \Omega$	$R_F = 15 \Omega$	$R_F = 25 \Omega$	$R_F = 70 \Omega$	$R_F = 0.02 \Omega$	$R_F = 15 \Omega$	$R_F = 25 \Omega$	$R_F = 70 \Omega$
2	2.009	2.011	2.012	2.014	0.45	0.55	0.60	0.70
5	5.021	5.028	5.037	5.038	0.42	0.56	0.74	0.76
10	10.006	10.006	10.006	10.007	0.65	0.67	0.69	0.74
20	20.013	20.014	20.015	20.020	0.67	0.72	0.79	1.04
40	40.028	40.029	40.030	40.038	0.72	0.72	0.75	0.97
50	50.035	50.038	50.041	50.049	0.70	0.77	0.82	0.98
70	70.055	70.057	70.058	70.069	0.79	0.81	0.84	0.99
80	80.068	80.072	80.074	80.088	0.85	0.90	0.93	1.10
85	85.076	85.082	85.084	85.099	0.89	0.97	0.99	1.17
90	90.085	90.092	90.094	90.088	0.95	1.03	1.04	1.21
95	95.091	95.097	95.099	96.016	0.96	1.02	1.05	1.22

V. CONCLUSION

A novel MFT based algorithm developed for fast and precise phasor estimation has been realized for high speed distance protection. The occurrence of high impedance fault is successfully detected with the proposed algorithm based on differential measurement. The performance of developed algorithm reveals that it identifies type of fault with classification accuracy of 100% with fault distance estimator error remains around 1%. Apart from accurate trip signal generation, the proposed algorithm can also calculate fault time, fault location

and type of fault which are very much helpful to protection engineers to achieve the desirable attributes of protective system.

APPENDIX

Generator Data:

Power rating: 210 MVA,

Voltage rating: 13.8 KV,

Power Factor: 0.8 lagging

Frequency = 50 Hz

Positive-sequence = $0.871 + j9.96$

Zero sequence impedance = $1.8 + j20$

Line Data:

Length = 120 km

Voltage = 220 kV

Positive sequence impedance = $0.03 + j0.35$ /km

Zero-sequence impedance = $0.2 + j1.5$ /km

Positive-sequence capacitance = 10 nF/km

Zero-sequence capacitance = 7 nF/km

REFERENCES

1. Technical Report, "Power System Transmission Challenges and Research Needs" EPRI Report, 2011.
2. Final Report, "U.S.-Canada Power System Outage", Task force, 2012.
3. Summary Report, "Grid Disturbance in India on 30th July, 2012", Technical Committee, 2012.
4. A. Sarwade, P. Katti, J. Ghodekar, "Adaptive solutions for distance relay settings," IPEC 2010.
5. S. Yu, J. Gu, "Removal of Decaying DC in Current and Voltage Signals using a Modified Fourier Filter Algorithm", IEEE Transactions on power delivery, Vol. 16, Issue 1, July 2001.
6. U. Patel, N. Chothani, P. Bhatt, "Auto-reclosing Scheme with Adaptive Dead Time Control for Extra High Voltage Transmission Line", IET Science Measurement and Technology, Vol. 12, Issue 8, Nov. 2018.
7. E. Schweitzer, D. Hou, "Filtering for protective relays", Western Protective Relay Conference, Spokane, WA, 2002.
8. G. Benmouyal, "Removal of decaying dc in current wave forms using digital mimic filtering", IEEE Transaction on power delivery, Vol. 10, April 1995.
9. M. Rosa, C. Fernandez, N. Nelson, D. Rojas, "An overview of wavelet transforms application in power systems," PCCC Power System Computation Conference, Spain, June 2002.
10. B. Mahamedi, "A new power swing blocking function based on wavelet transform" Electric Power and Energy Conversion Systems, Vol. 14, Issue 1, 2011.
11. H. Mohammed, H. Musa, H. Zhengyou, F. Ling, Y. Deng, "A cumulative standard deviation sum based method for high resistance fault identification and classification in power transmission lines," Protection and control of modern power systems, 2018.
12. H. Jiali, D. Yuqian, L. Yongli, W. Gang, L. Shanshan, "Distance relay protection based on artificial neural network," Advances in Power System Control, Operation and Management, 1997.
13. U. Patel, N. Chothani, P. Bhatt, "Sequence-space-aided SVM classifier for disturbance detection in series compensated transmission line", IET Science Measurement and Technology, Vol. 12, Issue 8, Nov. 2018.
14. E. Feilat, K. Al-Tallaq, "A new approach for distance protection using artificial neural network," Universities Power Engineering Conference, 2004.
15. X. Lin, H. Weng, H. Liu, W. Lu, P. Liu, Z. Bo, "A novel adaptive single-phase reclosure scheme using dual-window transient energy ratio and mathematical morphology," IEEE Transaction on Power Delivery, Vol. 21, Issue 4, Oct. 2006.